

Experimental and numerical investigation of the aerodynamic interactions between a hovering helicopter and surrounding obstacles

Q. Gallas, ONERA - The French Aerospace Lab., F-59014 Lille, France, quentin.gallas@onera.fr

R. Boisard, ONERA - The French Aerospace Lab., F-92190 Meudon, France

J.-C. Monnier, ONERA - The French Aerospace Lab., F-59014 Lille, France

J. Pruvost, ONERA - The French Aerospace Lab., F-59014 Lille, France

A. Gilliot, ONERA - The French Aerospace Lab., F-59014 Lille, France

Abstract

This paper presents the work carried out by the Aerodynamics Aeroelasticity and Acoustics Department of ONERA in the framework of the GARTEUR (Group for Aeronautical Research and Technology in Europe) Action Group 22 "Forces on Obstacles in Rotor Wake". The ONERA activities consist in two tasks performed in parallel, both presented in this paper. It first consists in an original experimental activity to study the aerodynamic interactions of a helicopter model placed in a square pit. The objective of this test campaign is to experimentally characterize the aerodynamic interactions between a helicopter and its surrounding. Experimental measurements include aerodynamic forces, wall static pressures, flow visualizations and Stereo-PIV in the field. The results help in the understanding of the complex flow phenomena encountered. Then since the boundary conditions of the experiment are well documented, the experimental database allows the validation of numerical tools, which is the second task presented in this paper. The objective of the numerical study is to validate the ONERA low fidelity tool PUMA by comparing its aerodynamic rotor loads prediction to the different available databases. PUMA tool is based on a lifting line approach coupled with a freewake model. The results show good agreement between the numerical findings and the experimental results and prove the ability of the PUMA tool to accurately simulate such a complex flow interaction mechanism.

1 NOMENCLATURE

Symbol	Description	Units
c	Chord length	m
C_p	Pressure coefficient	
Ω	Rotor rotation speed	RPM
D	Rotor diameter	m
R	Rotor radius	m
u, v, w	Velocity components	m/s
x, y, z	Geometrical coordinates	m
Δp	Pressure difference wrt p_∞	Pa
Θ_0	Collective pitch	deg
μ	Advance ratio	
σ	Rotor solidity	
HIGE	Hover In Ground Effect	
HOG E	Hover Out of Ground Effect	

2 INTRODUCTION

Helicopters are adaptable flying machines that are often required to operate in confined areas or close to obstacles in stationary motion. The knowledge of the aerodynamics interactions occurring between the rotating rotor and the surroundings is therefore of great interest for safety, maneuverability and design issues. This subject has become a promising research topic in the rotorcraft community. In particular, within the framework of the GARTEUR (Group for Aeronautical Research and Technology in Europe) Action Group 22 "Forces on Obstacles in Rotor Wake" [1], several research institutes and universities in Europe have gathered their strength to work on this subject. This GARTEUR group involves

universities (Politecnico di Milano, University of Glasgow, National Technical University of Athens) and research institutes (ONERA, CIRA, DLR, NLR). The work carried out by the Aerodynamics, Aeroelasticity and Acoustics Department of ONERA is presented in this paper.

The ONERA activities consist in two tasks performed in parallel, which are both presented in this paper. It first consists in an original experimental activity to study the aerodynamic interactions of a helicopter model placed in a square pit. The first objective of this test campaign is to experimentally characterize the aerodynamic interactions between a helicopter and its surrounding, as shown in Figure 1. Experimental measurements include aerodynamic forces, wall static pressures and stereo-PIV (SPIV) in the field. Tests are performed with a small scale helicopter Sphynx 3D fastened to a balance to measure the six components of the aerodynamic forces generated by the rotor in presence of a ground and a well-shaped obstacle. In the experiment, the similarity rules for extrapolation to real and large helicopters were not fully respected (Reynolds number, compressibility effects and blade kinematics). Then since the boundary conditions of the experiment are well documented, the experimental database allows validation of numerical tools, which is the second objective of the study.



Figure 1: ONERA experiment: helicopter mounted in a square-shaped box representing a closed courtyard

The second ONERA activity within GARTEUR AG22 consists in reproducing numerically different experiments performed within this project. The objective of the numerical study is to validate ONERA free-wake tool (known as PUMA) by comparing its aerodynamic rotor loads prediction to the different available databases. PUMA tool is based on a lifting line approach coupled with a freewake model and is already extensively used and validated at ONERA for a wide range of rotating blades applications (propeller, open rotors, helicopter rotor and wind turbine). However, the capability to account for any obstacle shape was recently developed and still need some validation. A first validation was performed within the GARTEUR AG22 against Polimi experiment with no wind [2]. Based on the success of these first computations, the current paper is devoted to the validation of PUMA against the ONERA experiment.

3 EXPERIMENTAL APPROACH

3.1 Test setup

The test rig is based on the commercial R/C helicopter model Sphynx 3D, including a rotor head with global and cyclic control in pitch. The helicopter has been strongly customized [3]: the tail rotor and the cyclic pitch were removed; a six components balance, an external energy supply, etc. were introduced. The rotor has two rectangular blades with NACA0012 airfoil, diameter $D = 0.71$ m and velocity $\Omega = 2600$ RPM. The collective pitch was set at a fixed angle $\theta_0 = 7.5^\circ$. The helicopter is mounted in the center of a square-shaped courtyard. The platform simulating a complete ground is at 1.2 m above the building floor. The walls have a parallelepiped form, are made with wood and screwed onto the floor. The interior sides of the walls are painted in black for visualizations and SPIV purposes. The wall is 0.36 m high with a thickness equal to 0.30 m.

The experimental setup is presented Figure 1 and Figure 2. It allows the helicopter to be translated above the floor, and the surrounding buildings can be removed. This permits comparison of HIGE and HOGE. Tests are conducted in free air in the aerodynamic laboratory of ONERA-Lille.

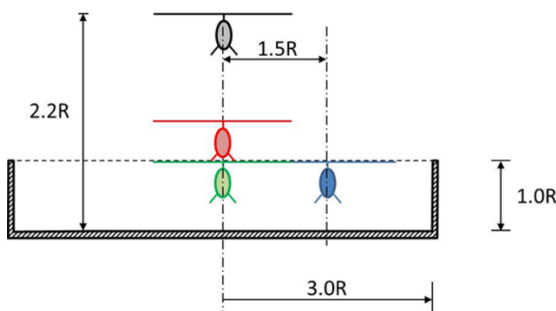


Figure 2: Layout of the ONERA test cases

3.2 Measurement setup

The measurement setup consists in the acquisition of four different sets. First, aerodynamic forces and moments on the rotor are measured via a 6-components balance. The acquisition of the balance signals is done at 2 kHz during

15 s with a high frequency filter at 1 kHz to eliminate the high frequencies folding. Careful attention has been paid on the integration of the aerodynamic balance in order to avoid any structural interference [3]. The nominal rotation rate for the tests is chosen at the frequency at which the vibrations are minimum and between the first and the second structural frequencies. The important coefficients are the mean thrust and the rotor torque. The tests are performed in hover condition.

Next, pressure measurements along the floor and the wall are realized using 9 Druck PDRCR42 of 75 mbars, flush-mounted on a rod alternatively inserted in the floor and in the side wall. The pressures were characterized in static (~ 5 s) with a MENSOR differential sensor with a guaranteed accuracy of 0.25 Pa on the scale ± 400 Pa.

Then, some flow visualizations are performed with a high speed video camera, a smoke generator and a laser light sheet aligned with the rotor head. These flow visualizations help in the understanding of the flow physics mechanism for the different configurations studied.

Finally, the test campaign includes Stereo-PIV measurements that are done in an area located below the rotor and on the advancing blade side of the model, as schematized Figure 3. Along the different tests cases presented Figure 2, only the test case shown in Figure 3 is measured in SPIV. The two PIV cameras as well as the laser are synchronized with one-per-rev signal provided by a sensor on the helicopter rotor. The acquisition frequency is set to 4.8 Hz, which is equivalent to one PIV recording for nine rotor revolutions. The PIV analysis is done with the in-house ONERA DaapPIV software. The image analysis is realized with a multi-pass intercorrelation FFT. The final window size is 32×32 pixels² with 50% overlap, which corresponds to a spatial resolution of 7.4×7.4 mm². 3500 pairs of images are acquired in total allowing a suitable convergence for the mean and fluctuating velocity components.

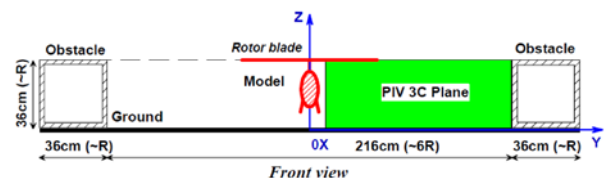


Figure 3: Configuration of the model and S-PIV area

3.3 Experimental results

This section presents the main results obtained during the ONERA test campaign.

First, the thrust measured with and without the presence of the obstacles is shown Figure 4. The ground effect becomes very small for $z/R > 2$, which is a classical result. However, one should note that the buildings decrease the effect of the ground. A test to check whether the helicopter fuselage has an effect on the aerodynamic coefficients is also performed, and results show that the effect of fuselage presence seems negligible.

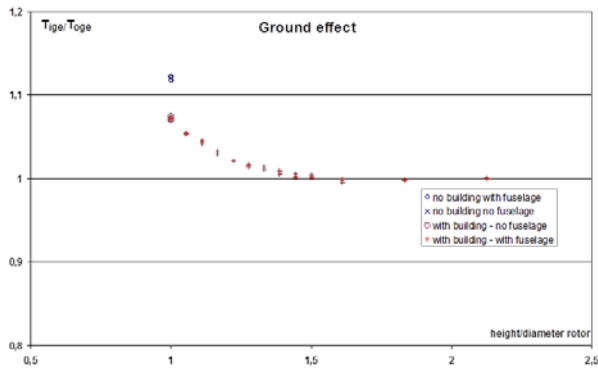


Figure 4: Ratio of the thrust with and without ground vs. the reduced height z/R .

The mean pressures on the ground obtained by different tests with and without the walls are next presented in Figure 5; the origin of the abscissa is the rotor axis of rotation. The blade tip location at 360 mm is marked on the figure with a dashed black line. A polynomial fitting is done for the two configurations assuming that the oscillations are random. The differences between the two curves, with and without the presence of the walls, are only significant at a distance from the rotor axis greater than 850 mm. There is overpressure of ~ 22 Pa under the rotor and a small under pressure ~ -5 Pa farther due to the velocity flow along the ground.

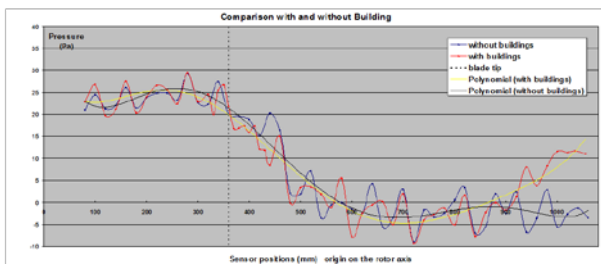


Figure 5: Pressure measurements on the ground with and without the side walls

Then, Figure 6 shows an extracted image of flow visualization. Here the field of view is focused on the blade tip, and the image is in direct negative color. The rotor head appears on the right-up side. The vortices shed at the extremity of the blades are well visible and their core, generated by the centrifugation of the smoke, grows rapidly at their birth. Near the ground the flow expand radially with rebounds of the vortices at different height.

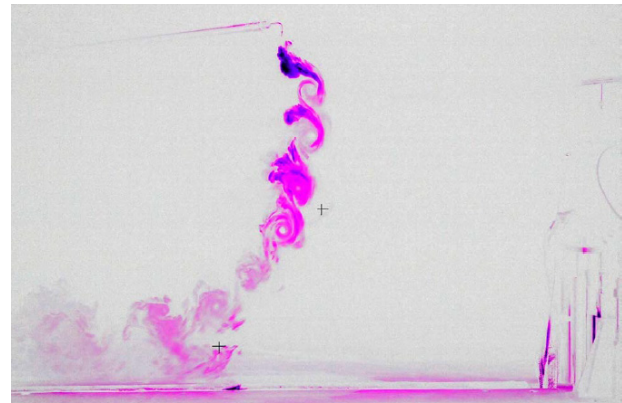


Figure 6: Smoke visualization of blade tip vortices

Such result from flow visualization can be directly compared with SPIV images. Figure 7 shows instantaneous PIV images recorded at 90° azimuthal angle where the blade is present in the top of the image. Because of the high vorticity of the vortices emitted by the blade tip, the vortex cores are not seeded (centrifugal effects), which let them visible in the images. While Figure 7 left shows the trajectory of vortex cores at one instant in time, similarly to Figure 6, Figure 7 right shows the spatial dispersion of the vortex cores during time. Note that Figure 6 is acquired in the retreating side of the blade and that Figure 7 is on the advancing side.

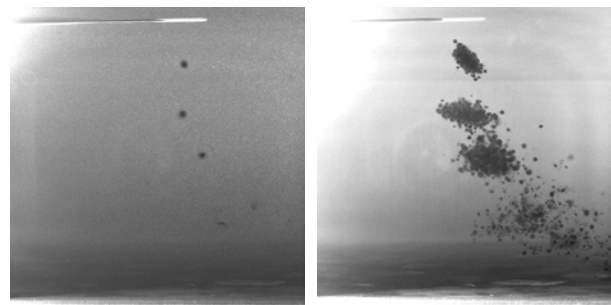


Figure 7: One instantaneous (left) and superimposed instantaneous (right) PIV recordings.

The PIV images can be further post-processed and analyzed in a phase-locked manner to yield the results presented in Figure 8 and Figure 9. The mean trajectory of the blade tip vortices are extracted from the SPIV images and are shown in Figure 8. The vortices follow the same path whatever the azimuthal blade position. Their time life is plotted in Figure 9, showing a high decay rate with a minimal persistence while they approach the floor, corresponding to findings from the flow visualizations and the static pressure results presented above.

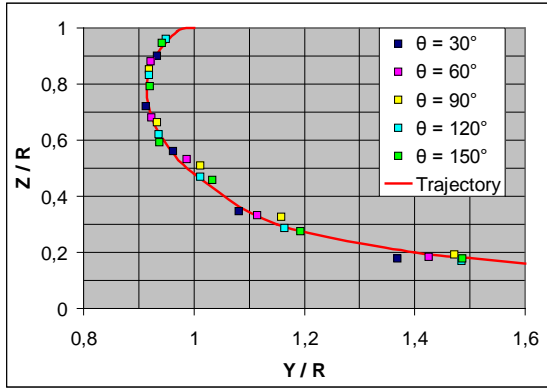


Figure 8: Trajectory of the blade tip vortices from S-PIV.

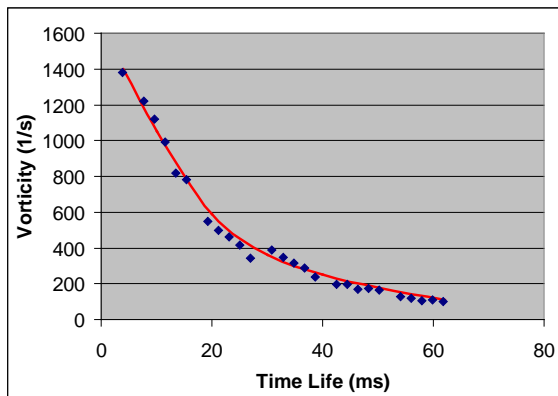


Figure 9: Blade tip vorticity magnitude function of their time life from S-PIV.

Figure 10 shows an example from the SPIV results of the mean flow field in between the helicopter and the surrounding walls. The blade tip vortices are convected downward and then translated towards the walls, before flowing up along the vertical walls. This mechanism forms a large recirculation bubble in the transversal direction, while an azimuthal flow velocity circulates inside the closed courtyard. The core of the recirculating region is located at $z/R = 1$ in the vertical axis, and in between the blade tip and the vertical wall in the longitudinal axis. Close to the rotor head, a chimney effect is put in evidence, as previously seen by the flow visualizations.

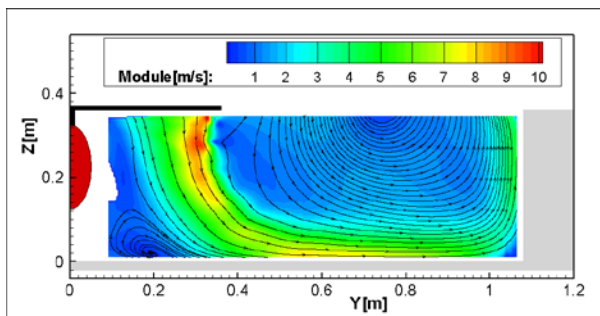


Figure 10: Mean velocity and streamlines for 90° blade position.

4 NUMERICAL APPROACH

4.1 Free wake method: PUMA

The PUMA (Potential Unsteady Methods for Aerodynamics) code, which is developed at ONERA since 2013, is based on a long lasting knowledge about free wakes methods for helicopter aerodynamics. It is built on a coupling between an aerodynamic module and a kinematic module. The aerodynamic module relies on a free wake model and a lifting line approach. The free wake model is based on Mudry theory [4] which rigorously describes the unsteady evolution of a wake modelled by a potential discontinuity surface. The lifting line method relies on 2D airfoils characteristics and can handle some 3D corrections for blade sweep and 2D unsteady aerodynamics effects through dynamics stall models. Moreover, different time discretizations are available in order to balance between accuracy, scheme stability and computational time. At last, influence of any arbitrary surface onto the wake can be taken into account using a potential approach. Concerning the kinematic module, it is based on a rigid multi-body system approach using a tree-like structure with links and articulations. In order to reduce computational time, the code has been parallelized using OpenMP and the Multilevel Fast Multipole Method has been implemented for the computation of the velocities induced by each wake panel on any element. PUMA has been validated against CFD computations and experiment for various configurations of rotating wings such as propellers, counter rotating open rotors, helicopter rotors and more recently wind turbines. It is now extensively used at ONERA for any aerodynamic study of fixed wings and rotating wings configurations which requires low computational cost or a large amount of parametric investigations like pre-design studies.

The NACA0012 airfoil data needed for the lifting line computations were computed using elsA CFD solver [5] for a constant Reynolds number over Mach number corresponding to the rotor scale.

Concerning the numerical parameters used for the computations, they are based on ONERA previous experience on the use of PUMA for helicopter rotors. The more meaningful parameters are:

- ✓ 16 radial stations for blade definition (note that the cylindrical part of the blade was not included in the computation)
- ✓ 25 radial stations for wake emission using square root distribution along the span
- ✓ Ground is taken in to account using a symmetry plane
- ✓ Building is taken into account using hexa unstructured grid
- ✓ 10° time steps
- ✓ 40 revolutions computed to ensure acceptable convergence, with an averaging of the rotor loads over the last 5 revolutions
- ✓ No modelling of the helicopter fuselage and test rig

4.2 Numerical results

Figure 13 shows the rotor load prediction using the free wake approach with and without the building. The rotor thrust was non dimensionalized using the thrust value without building, and numerical results were averaged of the last 5 rotor revolution to smooth the highly unsteady loads. Without the building, the computation, forecast a reduction of thrust as the rotor is moving away from the

ground, which is perfectly in line with what is expected for a rotor operating in 'simple' ground effect. With the building a similar behavior is observed, but with a lower value of thrust (roughly 3%) than the one observed without the building. This results almost match the experiment with predict a 4% decrease of thrust with the building. It should be noticed that these relatively good results are obtained only when 20 rotor revolution are kept in the wake to compute the induced velocity on the rotor blades. If only accounting for 10 rotor wake revolutions, there is almost no difference with and without the building.

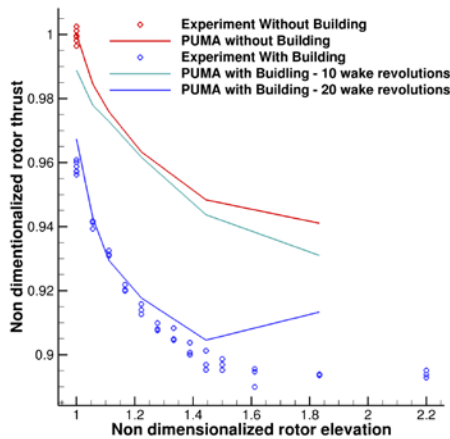


Figure 11: Building effect on rotor loads using free wake approach

As it is seen in Figure 14, using only 10 rotor wakes revolution, the flow around the rotor is almost exactly the same with and without the building. It is due to the fact that the rotor wake takes a very long time to reach the building wall and rise along them. It takes at least 20 rotor revolution for the wake to reach the top of the building wall and interact with the flow above the rotor disc. Doing so, the rotor wake lowers the rotor inflow velocity reducing the rotor thrust.

While increasing the number of rotor wake kept in order to compute the induced velocity could be expected to improve the comparison with experiment, it was actually not the case. It only drastically increases the unsteadiness of the loads. It can be seen that keeping 30 wake revolution leads to some spot of high velocity in the flowfield that will be re-interacting with the rotor blades. This is one limitation of such free-wake methods. Since there is no dissipation of the wake, in such configuration with re-entering flow, the rotor wake is stronger than it should be at the time it re-interacts with the blades. This kind of issues were not observed for simple ground effects computations, and also rotor / building interaction that do not involved re-entering flows as in Polimi experiment [2]. Figure 15 shows a comparison of the induced velocity modulus in the wake with the PIV measurements for a rotor blade at 0° azimuth. The overall behavior is relatively well captured, with a recirculating region located between the rotor center and the building wall. However, in the experiment, this recirculating region is larger than in the computation. In the computation some secondary recirculating region are also located in the rotor wake near the tip vortices path. It is expected to be due to the lake of wake and tip vortices dissipation in the computation.

The chimney effect that was observed in experiment is also observed in the computation however, once again, it feature some strong velocity spots that are not seen in experiment. This is once again due to the lake of dissipation in the computation and also to the fact that the rotor hub is not modelled leading to some strong blade root vortex that do not exist in the experiment.

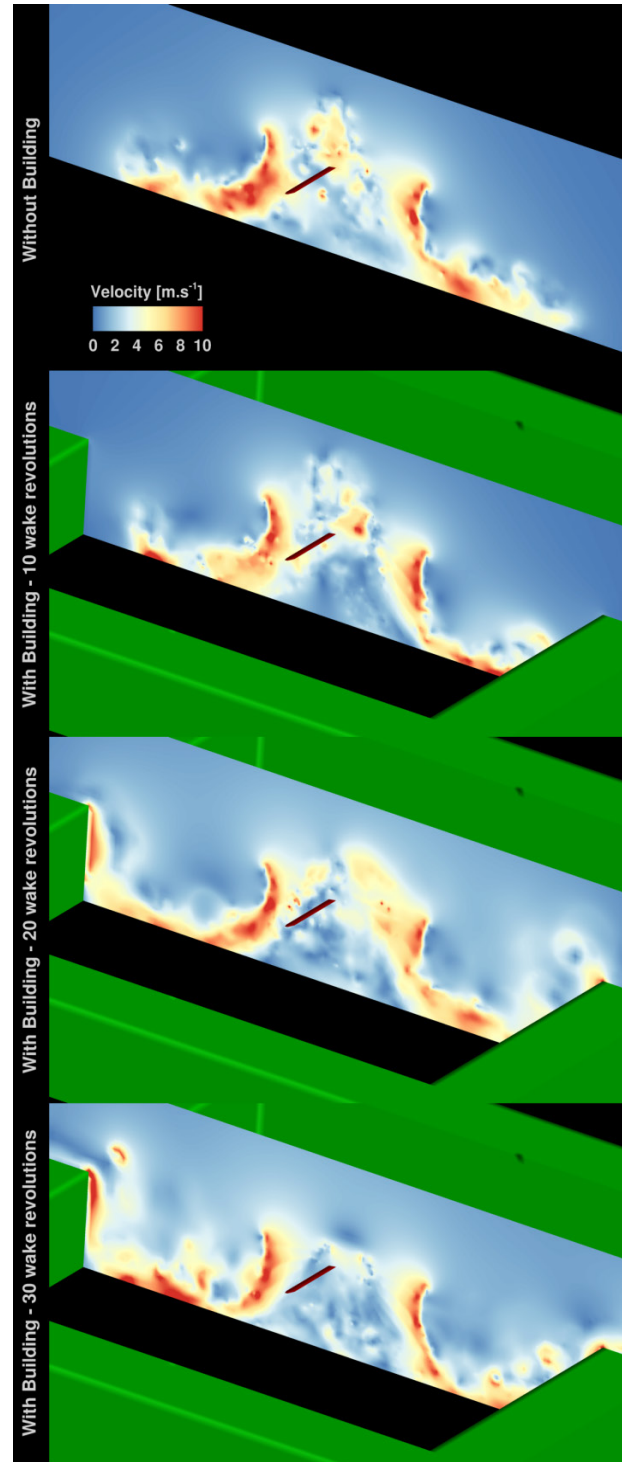


Figure 12: Building effect on rotor wake using free wake approach

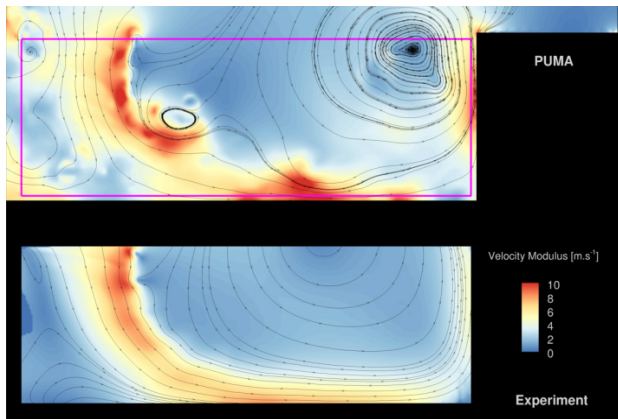


Figure 13: Velocity modulus in the PIV plane for 0° blade position using free wake approach

5 CONCLUSIONS

An original hovering helicopter case has been presented in this paper, dealing with helicopter hovering in a confined area. The paper presented the work performed by ONERA within the GARTEUR Action Group 22 "Forces on Obstacles in Rotor Wake". It contains both an experimental and a numerical activity. The experimental work consists in measuring the aerodynamic loads on the rotor head of a helicopter test model in proximity of a closed square courtyard, in HIGE and HOGÉ conditions. Static pressure measurements, flow visualizations and Stereo-PIV measurements completed the experimental dataset. Both pressure and PIV data provide local measurements in the field, while the aerodynamic forces provide global findings. These measurements bring a better understanding in the flow dynamics of the wake/obstacle interaction.

This experimental dataset is also used as a validation database for ONERA low fidelity tool (known as PUMA) by comparing the aerodynamic rotor loads prediction. The results show that such low fidelity approach is perfectly able to capture overall effect of the obstacle on the rotor performances. However, such approach has some limitation mainly due to the lack of dissipation of the wake which is re-entering the rotor disc. CFD computation may be mandatory to accurately capture the local details of the flowfield.

Future work will be devoted to further analyze the experimental database. Other numerical tools from GARTEUR AG22 partners will be validated against the ONERA experimental database including some CFD computations performed at ONERA.

6 ACKNOWLEDGMENTS

Some equipment used in the present communication has been supported by the regional platform CONTRAERO in the framework of the CPER ELSAT 2020 Project. The ELSAT 2020 project is co-financed by the European Union with the European Regional Development Fund, by the French State and the Hauts de France Region under the State Region Contracts (CPER).

7 REFERENCES

[1] White, M., "GARTEUR General Presentation and Research Activities of the Helicopter Group" 42nd

- European Rotorcraft Forum, September 5-8 2016, Lille, France
- [2] G. Gibertini, D. Grassi, C. Parolini, D. Zagaglia, A. Zanotti, "Experimental investigation on the aerodynamic interaction between a helicopter and ground obstacles," Proceedings of the Institution of Mechanical Engineers, Part G: Journal of Aerospace Engineering June 2015 229: 1395-1406, first published on September 21, 2014
- [3] Paquet JB, Bourez JP, Morgand S., « Formulation of Aerodynamic Forces on Helicopters in Non Uniform Flow with Scale Model Tests: Ground Effects", 49th International Symposium of Applied Aerodynamics, Lille, 24-25-26 March 2014.
- [4] Mudry, M., "La théorie des nappes tourbillonnaires et ses applications à l'aérodynamique instationnaire", Thèse de Doctorat d'état, Université Paris VI, July 1982
- [5] L. Cambier, S. Heib, S. Plot, "The Onera elsA CFD software: input from research and feedback from industry," Mechanics & Industry, 14, pp 159-174, 2013